Indonesian Journal of Electrical Engineering and Computer Science
Vol. 41, No. 3, March 2026, pp. 924∼934
ISSN: 2502-4752, DOI: 10.11591/ijeecs.v41.i3.pp924-934

Mobility-aware adaptive tag selection strategy in ambient backscatter systems

Mengistu Abera Mulatu[1], Thembelihle Dlamini[1], Wiseman Nkosingiphile Nyembe[1], Zenzo Polite Ncube[2], Asrat Mulatu Beyene[3]
[1]Department of Electrical and Electronic Engineering, University of Eswatini, Kwaluseni, Eswatini
[2]Department of Computer Science, University of Eswatini, Kwaluseni, Eswatini
[3]Department of Electrical and Computer Engineering, Addis Ababa Science and Technology University, Addis Ababa, Ethiopia

Article Info

Article history:

Received Oct 3, 2025
Revised Jan 21, 2026
Accepted Feb 27, 2026

Keywords:

Backscatter communication
IoT
Mobile receiver
Passive tags

ABSTRACT

Ambient backscatter communication (AmBC) has emerged as a promising solution to enable ultra-low-power connectivity in large-scale internet of things (IoTs) and future 6G mobile networks. In this paper, we consider a mobility-aware AmBC system, where a mobile user equipped with a reader interacts with multiple passive tags deployed in the coverage area of a base station (BS). To achieve high decoding reliability, an adaptive tag selection scheme is proposed based on received signal strength (RSS) and interference constraints. Here, we derive a closed-form expression of the outage probabilities of both the mobile user and tags taking into account the Rayleigh double-fading nature of backscatter links. Performance evaluation carried out through simulations validates the theoretical analysis based on various selected system parameters. The results obtained show that the proposed adaptive scheme significantly improves system reliability compared to fixed tag selection strategies, thus emphasizing the importance of mobility-aware and context-driven adaptation in mobile IoT scenarios such as smart transportation and aerial data collection.

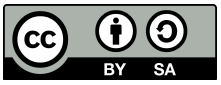

Corresponding Author:

Mengistu Abera Mulatu
Department of Electrical and Electronic Engineering, University of Eswatini
Kwaluseni, Eswatini
Email: mamulatu@uneswa.ac.sz

1. INTRODUCTION

The rapid growth of applications for the internet of things (IoT) and the growing demands of 5G, B5G, and future 6G networks have significantly increased the demand for communication technologies that are energy-efficient and spectrally efficient [1]. As the number of connected devices increases, the demand for low-power, scalable, and spectrum efficient communication systems is more demanding than ever. Currently, traditional wireless communication methods are not able to handle the expected massive device connections as they were not designed for that.

To handle the increase in device connections, ambient backscatter communication (AmBC) has emerged as a promising solution in this space due to its ability to enable battery-free devices to communicate by modulating and reflecting existing ambient radio frequency (RF) signals. This approach is able to handle the energy limitations faced by large-scale IoT deployments and boosts spectral efficiency by making use of the existing RF infrastructure for dual-purpose communication [2]-[5]. In AmBC systems, passive tags transmit their messages by reflecting modulated versions of ambient signals coming from sources like cellular

base stations (BS), Wi-Fi access points, or TV towers without the need for dedicated power supplies. Despite its benefits for large-scale IoT deployments, signal detection in AmBC remains challenging due to three main factors: (i) the weak nature of backscattered signals, (ii) the presence of double-fading channel effects, and (iii) co-channel interference in environments with multiple coexisting devices [6].

Recent works have addressed these limitations by proposing architectural enhancements to improve reliability and spectral efficiency. Cooperative AmBC systems and backscatter non-orthogonal multiple access (NOMA) architectures have demonstrated enhanced spectral efficiency and improved support for massive connectivity [7]-[9]. For instance, the work of [10] investigated a NOMA-based symbiotic radio (SR) system, deriving exact and asymptotic outage probabilities under Nakagami-m fading. Their results showed that power-domain multiplexing combined with successive interference cancellation (SIC) is effective in jointly decoding direct and backscattered signals. Moreover, Toro *et al.* [11] showed that intelligent reflecting surfaces (IRS) can further enhance AmBC performance by dynamically shaping the propagation environment. In addition, the integration of machine learning techniques have improved the system adaptability in dense IoT environments by optimizing tag-user association strategies [12], [13].

Despite the proposed strategies, one inherent limitation still exists in AmBC research work. Majority of the works assume static receivers and fixed tag configurations. This assumption overlooks practical deployment scenarios involving mobile receivers such as smartphones, drones, or vehicles that interact with ambient tags. For example, in a dense and mobile IoT deployments, the mobility of users and/or tags introduces dynamic variations in channel gains, interference, and energy harvesting conditions.

Traditional models that assume static user configurations [14]-[19] are insufficient to capture these dynamics. Therefore, adaptive tag selection and resource allocation are critical to address mobility-induced challenges. To bridge this gap, in this paper, we propose a novel adaptive tag selection scheme for AmBC systems with mobile receiver taking into account the received signal strength (RSS) and interference constraints. To clearly highlight the novelty and scope of this work, the main contributions of the paper are summarized as follows:

- We develop a mobility-aware AmBC framework with a mobile reader, where user mobility is explicitly modeled and its effects on channel variations, RSS, and interference are taken into account.
- We propose an adaptive RSS and interference-aware tag selection algorithm that dynamically selects a feasible subset of tags to satisfy decodability and SIC constraints under time-varying channel conditions.
- We derive closed-form expressions for the outage probabilities of both the mobile user and the selected tags by accounting for Rayleigh double-fading backscatter channels and mobility-induced dynamics.
- We validated the analytical derivations through Monte-Carlo simulations and carry out a comparison between the proposed system, the static users case and an orthogonal multiple access (OMA) based benchmark system.
- We demonstrate that the proposed adaptive tag selection scheme outperforms fixed tag selection strategies, thereby emphasizing the importance of mobility-aware and context-driven adaptation for future large-scale IoT and 6G-enabled ambient backscatter networks.

The remainder of this paper is organized as follows: the system model is introduced in section 2. Section 3 details the proposed adaptive tag selection algorithm. In section 4 provides the analytical performance derivation of outage probabilities. In section 5 discusses the numerical results, and finally section 6 concludes the paper.

2. SYSTEM MODEL

We consider an AmBC system consisting of a BS, N passive tags, and a mobile user. The BS transmits an RF signal with power P, which is simultaneously received by the user and reflected by the tags. The main system parameters and notations are summarized in Table 1. The BS and the tags are static, while the user moves continuously within the region based on a 2D mobility model (e.g., Linear Constant Velocity). The BS constantly transmits an ambient RF signal $\sqrt{P}x(t)$. Each tag T_k modulates this signal through backscattering with reflection coefficient β_k to embed its information onto the ambient signal.

Table 1. System parameters and descriptions

Parameter	Description
P	Transmit power of the ambient RF source (base station)
$x(t)$	Normalized baseband signal
$\mathcal{S}$	Set of adaptively selected active tags
$\lvert\mathcal{S}\rvert$	Number of selected (active) backscatter tags
β_k	Reflection coefficient of the k-th backscatter tag, $0 < \beta_k \leq 1$
$h_0(t)$	Channel coefficient between the base station and the mobile user
h_k	Channel coefficient between the base station and the k-th tag
$g_k(t)$	Channel coefficient between the k-th tag and the mobile user
$c_k(t)$	The backscattered symbol from the k-th tag
$v(t)$	Velocity of the mobile user
$d_0(t)$	Distance between the base station and the mobile user
$d_{h_k}(t)$	Distance between the base station and the k-th tag
$d_{g_k}(t)$	Distance between the k-th tag and the mobile user
α	Path-loss exponent
σ^2	Noise power at the mobile user receiver
$\gamma_u(t)$	Received SINR at the mobile user
$\gamma_{T_k}(t)$	SINR of the k-th backscatter tag under SIC
γ_{ut}	SINR threshold required for successful decoding of the user signal
γ_{Tt}	SINR threshold required for successful decoding of a tag signal

At any time t, the user's position is represented by $\mathbf{u}(t)$. It selects $K(t) < N$ tags for communication based on RSS. The user receives both the direct signal from the BS and the backscattered signals from a subset of $K(t)$ active tags. The composite received signal at the user at time t is given by:

$$y(t) = \sqrt{P}h_0(t)x(t) + \sum_{k=1}^{K(t)} \sqrt{P\beta_k}h_k g_k(t)x(t)c_k(t) + n(t), \tag{1}$$

where $n(t)$ is additive white Gaussian noise (AWGN) with zero mean and variance σ^2.

We assume that the channel coefficients are independent and identically distributed (i.i.d.) complex Gaussian random variables with zero mean and unit variance, with the corresponding channel power gains that follow an exponential distribution. Considering the Rayleigh fading assumption with distance-dependent path loss, the channel power gains are modelled as $|h_0(t)|^2 \sim \exp(\lambda_0(t))$, $|h_k|^2 \sim \exp(\lambda_{h_k})$ and $|g_k(t)|^2 \sim \exp(\lambda_{g_k}(t))$, where $\lambda_0(t) = d_0^{-\alpha}(t)e^{-\tau v(t)}$, $\lambda_{h_k} = d_{h_k}^{-\alpha}$ and $\lambda_{g_k}(t) = d_{g_k}^{-\alpha}(t)e^{-\tau v(t)}$. Note that the user mobility is incorporated via velocity-dependent path loss.

We assume that the channel state information is known to the tags using either the pilot signals or the blind channel estimation [20], [21] and the user implements SIC to decode its own message $x(t)$ first by treating the backscattered signals as interference . Upon successful demodulation, it subtracts $x(t)$ from the received signal and attempts to decode tag's information signal $c_k(t)$ sequentially based on their RSS. The instantaneous signal-to-interference-plus-noise ratio (SINR) of the user to decode $x(t)$ can be written as:

$$\gamma_u(t) = \frac{P|h_0(t)|^2}{\sum_{k=1}^{K(t)} P\beta_k|h_k|^2|g_k(t)|^2 + \sigma^2} \tag{2}$$

after decoding $x(t)$, the SINR for decoding the k-th tag's signal $c_k(t)$ is given by:

$$\gamma_{T_k}(t) = \frac{P\beta_k|h_k|^2|g_k(t)|^2}{\sum_{j\neq k}^{K(t)} P\beta_j|h_j|^2|g_j(t)|^2 + \sigma^2} \tag{3}$$

tags are decoded sequentially in descending RSS order. After each step, stronger tags are cancelled, leaving only weaker tags as residual interference.

3. ADAPTIVE TAG SELECTION ALGORITHM

In the this section, we propose a mobility-aware adaptive tag selection algorithm based on RSS and probabilistic interference constraints. The user mobility introduces dynamic variations in channel conditions, requiring adjustment of the number of active tags. The user selects a subset of tags $K(t)$ at time t based on the RSS, interference constraints and spatial distribution. In other words, only those tags whose RSS exceeds a predefined threshold (r_{th}) are considered. The expected number of selected tags is proportional to the overlapping coverage area between the user and the tags, and it is given as [22]:

$$\mathbb{E}[K(t)] = \rho \cdot A_{\text{overlap}}(t) e^{-\tau v(t)} \tag{4}$$

where ρ is the tag density, $A_{overlap}(t)$ is the overlap area between the user's interrogation zone and the tag's response range and τ is a penalty coefficient. In (4) implies that the number of readable tags varies with both tag density, the size of the overlapping coverage area and speed of the user.

To maintain the user's SINR above a threshold γ_{ut}, the total interference $I(t)$ from the selected tags must also be bounded, i.e., $I(t)$ from selected tags must not exceed a time-varying threshold $\epsilon(t)$. Using the Chernoff bound [23], we write the relationship as:

$$\mathbb{P}(I(t) > \epsilon(t)) \leq e^{-s\epsilon(t)} \mathbb{E}[e^{sI(t)}] \tag{5}$$

where $s > 0$ is a free parameter optimized to tighten the bound. For exponentially distributed interference $I_k(t) \sim \text{Exp}(\lambda_k(t))$, the moment-generating function (MGF) is $\mathbb{E}[e^{sI(t)}] = \frac{\lambda_k(t)}{\lambda_k(t)-s}$. For $K(t)$ tags, we have:

$$\mathbb{E}[e^{sI(t)}] = \prod_{k=1}^{K(t)} \frac{\lambda_k(t)}{\lambda_k(t) - s}, \; s < \min_k \lambda_k(t) \tag{6}$$

the optimal s^* is found by solving:

$$s^* = \arg\min_s \left(-s\epsilon(t) + \sum_{k=1}^{K(t)} \log\left(\frac{\lambda_k(t)}{\lambda_k(t) - s} \right) \right) \tag{7}$$

Interference minimization with decodability: The user suffers interference from the tags and selecting tags that minimize interference helps to improve the user SINR. However, if a tag signal is too weak, it cannot be decoded using SIC. Therefore, we impose a decodability threshold on each tag's signal strength to balance interference reduction and also to ensure that the tag signals are strong enough to be decoded. We define the double-fading channel strength of tag $\mathrm{T_k}$ as: $z_k(t) = |h_k|^2 |g_k(t)|^2$. The interference from tag $\mathrm{T_k}$ is $I_k(t) = \beta_k z_k(t)$. In order to decode a tag using SIC, its SINR must satisfy:

$$\text{SINR}_{T_k} = \frac{P\beta_k z_k(t)}{\sigma^2} \geq \gamma_{\text{Tkt}} \Rightarrow z_k(t) \geq \frac{\gamma_{\text{Tkt}} \sigma^2}{P\beta_k} = z_{\min} \tag{8}$$

After the selection of the K tags, the user feedbacks the signal to not more than $\log_2 \mathrm{N}$ bits to the tags, in order to notify the tags which can backscatter their messages and make the other tags keep silent [24]. The overall system has a per-slot computational cost of $\mathcal{O}(N \log N)$ mainly dominated by the tag selection stage. For a more detailed tag selection process, see Algorithm 1.

Algorithm 1. Tag selection algorithm

Require: Initialize, N, $z_{\min}$, $K(t)$
Ensure: Selected tag subset $\mathcal{T}_{\text{sel}}$

1. Initialize feasible tag list $\mathcal{F} \leftarrow \emptyset$
2. **for** each tag $k = 1$ to N **do**
3. Estimate h_k, $g_k(t)$ (e.g., using pilot signals or blind channel estimation)
4. Compute $z_k(t) = |h_k|^2 |g_k(t)|^2$
5. **if** $z_k(t) \geq z_{\min}$ **then**
6. Compute interference metric $I_k(t) = \beta_k z_k(t)$
7. Add $(k, I_k(t))$ to $\mathcal{F}$
8. **end if**
9. **end for**
10. Sort $\mathcal{F}$ in ascending order of $I_k(t)$
11. Select the top K tags from $\mathcal{F}$ to form $\mathcal{T}_{\text{sel}}$
12. **return** $\mathcal{T}_{\text{sel}}$

4. OUTAGE PERFORMANCE ANALYSIS

In the section, we evaluate the perofrmance of our prposed system by deriving the outage probabilities of both the mobile user and the selected backscatter tags by incorporating the time-dependent nature of the wireless channels due to user mobility. The channels between the BS and tags remain static, and channels associated with the user vary with time.

4.1. Outage probability of the user

The user experiences an outage when it cannot decode its own message $x(t)$ due to low SINR. An outage occurs when $\gamma_u(t) < \gamma_{ut}$, where $\gamma_{ut} = 2^{R_u} - 1$ is the SINR threshold corresponding to the user's target rate R_u. The outage probability of the user $P_{\text{out,u}}(t)$ is calculated as:

$$P_{\text{out,u}}(t) = 1 - \underbrace{\Pr(\gamma_u(t) \geq \gamma_{ut})}_{I_1} \tag{9}$$

Theorem 1. The closed form expression of $P_{\text{out,u}}(t)$ is given as:

$$P_{\text{out,u}}(t) = 1 - e^{-\frac{\gamma_{ut}\sigma^2}{\lambda_0(t)P}} \prod_{k=1}^{K(t)} \left[\frac{2\lambda_0(t)}{\gamma_{ut}\beta_k\lambda_{h_k}\lambda_{g_k}(t)} e^{\frac{\lambda_0(t)}{\gamma_{ut}\beta_k\lambda_{h_k}\lambda_{g_k}(t)}} \cdot \text{Ei}\left(\frac{-\lambda_0(t)}{\gamma_{ut}\beta_k\lambda_{h_k}\lambda_{g_k}(t)} \right) \right] \tag{10}$$

where, $\text{Ei}(\cdot)$ denotes the exponential integral function [9].

Proof: Using the expression for $\gamma_u(t)$ from (2) and with minor rearrangement, I_1 can be written as:

$$\begin{aligned} I_1 &= \Pr(|h_0(t)|^2 \geq \gamma_{ut}(\sum_{k=1}^{K} \beta_k z_k(t) + \sigma^2/P)) \\ &= \int_0^\infty \int_d^\infty f_{|h_0|^2}(x) f_{Z_k}(z_k(t)) dx dz_k(t) \\ &= e^{-\frac{\gamma_{ut}\sigma^2}{\lambda_0(t)P}} \int_0^\infty e^{-\frac{\gamma_{ut}}{\lambda_0(t)}\sum_k \beta_k z_k(t)} f_{Z_k}(z_k(t)) dz_k(t) \end{aligned} \tag{11}$$

where, $d = \gamma_{ut}(\sum_k \beta_k z_k(t) + \sigma^2/P)$, $f_{|h_0(t)|^2}(x) = \frac{1}{\lambda_0(t)} e^{-x/\lambda_0(t)}$, $f_{|h_k|^2}(y) = \frac{1}{\lambda_{h_k}} e^{-y/\lambda_{h_k}}$, $f_{|g_k(t)|^2}(w) = \frac{1}{\lambda_{g_k}(t)} e^{-w/\lambda_{g_k}(t)}$ and the probability density function (PDF) of $z_k(t)$ is given by $f_{Z_k}(z_k(t)) = \frac{2}{\lambda_{h_k}\lambda_{g_k}(t)} \cdot K_0\left(2\sqrt{\frac{z_k(t)}{\lambda_{h_k}\lambda_{g_k}(t)}}\right)$. Where $K_0(\tau)$ is the modified Bessel function of the second kind [25]. Substituting this in to (10) and performing rearrangement, we obtain:

$$I_1 = e^{-\frac{\gamma_{ut}\sigma^2}{\lambda_0(t)P}} \int_0^\infty e^{-\frac{\gamma_{ut}}{\lambda_0(t)}\sum_k \beta_k z_k(t)} \frac{2}{\lambda_{h_k}\lambda_{g_k}(t)} K_0\left(2\sqrt{\frac{z_k(t)}{\lambda_{h_k}\lambda_{g_k}(t)}}\right) dz_k(t). \tag{12}$$

Let $\tau = 2\sqrt{\frac{z_k(t)}{\lambda_{h_k}\lambda_{g_k}(t)}}$, from which $z_k(t) = \frac{\lambda_{h_k}\lambda_{g_k}(t)}{4}\tau^2$ and $dz_k(t) = \frac{\lambda_{h_k}\lambda_{g_k}(t)}{2}\tau d\tau$. After substitution and minor manipulations on the integral, we have:

$$I_1 = e^{-\frac{\gamma_{ut}\sigma^2}{\lambda_0(t)P}} \prod_{k=1}^{K(t)} \int_0^\infty \tau e^{-W\tau^2} K_0(\tau) d\tau \tag{13}$$

where, $W = \frac{\gamma_{ut}\beta_k\lambda_{h_k}\lambda_{g_k}(t)}{4\lambda_0(t)}$

$$I_1 = e^{-\frac{\gamma_{ut}\sigma^2}{\lambda_0(t)P}} \prod_{k=1}^{K(t)} \left[\frac{2\lambda_0(t)}{\gamma_{ut}\beta_k\lambda_{h_k}\lambda_{g_k}(t)} e^{\frac{\lambda_0(t)}{\gamma_{ut}\beta_k\lambda_{h_k}\lambda_{g_k}(t)}} \cdot \text{Ei}\left(\frac{-\lambda_0(t)}{\gamma_{ut}\beta_k\lambda_{h_k}\lambda_{g_k}(t)} \right) \right] \tag{14}$$

therefore, the outage probability of the user is given as:

$$P_{\text{out,u}}(t) = 1 - e^{-\frac{\gamma_{ut}\sigma^2}{\lambda_0(t)P}} \prod_{k=1}^{K(t)} \left[\frac{2\lambda_0(t)}{\gamma_{ut}\beta_k\lambda_{h_k}\lambda_{g_k}(t)} \cdot e^{\frac{\lambda_0(t)}{\gamma_{ut}\beta_k\lambda_{h_k}\lambda_{g_k}(t)}} \cdot \text{Ei}\left(\frac{-\lambda_0(t)}{\gamma_{ut}\beta_k\lambda_{h_k}\lambda_{g_k}(t)} \right) \right] \tag{15}$$

4.2. Outage probability of the tags

A tag $\mathrm{T_k}$ is in outage if either the user fails to decode $x(t)$ or successfully decodes $x(t)$ but fails to decode $c_k(t)$. Therefore, the outage probability is written as:

$$P_{out,T_k}(t) = 1 - \underbrace{\Pr\left(\gamma_u(t) \geq \gamma_{ut}, \gamma_{T_k}(t) \geq \gamma_{Tt}\right)}_{I_2} \tag{16}$$

where $\gamma_{Tt} = 2^{R_T} - 1$ for the tag's target rate R_T.

Theorem 2. The closed form expression of $P_{out,T_k}(t)$ is given as:

$$P_{out,T_k}(t) = 1 - I_1 + I_3. \tag{17}$$

where, I_1 is given in (14) and

$$I_3 = \frac{\pi\gamma_{Tt}}{M}\left(\sum_{j\neq k}\beta_j|h_j|^2|g_j(t)|^2 + \frac{\sigma^2}{P}\right)e^{-\frac{\gamma_{ut}\sigma^2}{\lambda_0(t)P}} \cdot \prod_{k=1}^{K(t)}\frac{1}{\lambda_{h_k}\lambda_{g_k}(t)}\sum_{m=1}^{M}\sqrt{1-\zeta_m^2} \tag{18}$$
$$\cdot\, e^{-\frac{\gamma_{ut}\beta_k\left(\sum_{j\neq k}\beta_j|h_j|^2|g_j(t)|^2+\sigma^2/P\right)\gamma_{Tt}(\zeta_m+1)}{2\lambda_0(t)}} \cdot K_0\left(\sqrt{\frac{2\gamma_{Tt}\left(\sum_{j\neq k}\beta_j|h_j|^2|g_j(t)|^2+\frac{\sigma^2}{P}\right)(\zeta_m+1)}{\lambda_{h_k}\lambda_{g_k}(t)}}\right)$$

Proof: Following similar outage analysis approach for user, I_2 can be written as:

$$I_2 = \Pr\Big\{|h_0(t)|^2 \geq \gamma_{ut}\Big(\sum_{k=1}^{K(t)}\beta_k z_k(t) + \frac{\sigma^2}{P}\Big), z_k(t) \geq \gamma_{Tt}\Big(\sum_{j\neq k}\beta_j z_j(t) + \frac{\sigma^2}{P}\Big)\Big\} \tag{19}$$
$$= \int_{A_1}^{\infty}\int_{A_2}^{\infty} f_{|h_0(t)|^2}(x)\, f_{Z_k}(z_k(t))\, dx\, dz_k(t) = e^{-\frac{\gamma_{ut}\sigma^2}{\lambda_0(t)P}}\int_{A_1}^{\infty} e^{-\frac{\gamma_{ut}}{\lambda_0(t)}\sum_k\beta_k z_k(t)} f_{Z_k}(z_k(t))\, dz_k(t)$$
$$= e^{-\frac{\gamma_{ut}\sigma^2}{\lambda_0(t)P}}\int_{0}^{\infty} e^{-\frac{\gamma_{ut}}{\lambda_0(t)}\sum_k\beta_k z_k(t)} f_{Z_k}(z_k(t))\, dz_k(t) - e^{-\frac{\gamma_{ut}\sigma^2}{\lambda_0(t)P}}\int_{0}^{A_1} e^{-\frac{\gamma_{ut}}{\lambda_0(t)}\sum_k\beta_k z_k(t)} f_{Z_k}(z_k(t))\, dz_k(t)$$

where $A_1 = \gamma_{Tt}(\sum_{j\neq k}\beta_j z_j(t) + \sigma^2/P)$ and $A_2 = \gamma_{ut}\left(\sum_{k=1}^{K(t)}\beta_k z_k(t) + \frac{\sigma^2}{P}\right)$. The first term of (19) is identical to (11) and its solution is given by (14). Define $I_3 = e^{-\frac{\gamma_{ut}\sigma^2}{\lambda_0(t)P}}\int_0^{A_1} e^{-\frac{\gamma_{ut}}{\lambda_0(t)}\sum_k\beta_k z_k(t)} \cdot f_{Z_k}(z_k(t))dz_k(t)$. Then we can write I_3 as:

$$I_3 = e^{-\frac{\gamma_{ut}\sigma^2}{\lambda_0(t)P}}\int_0^{A_1} e^{-\frac{\gamma_{ut}}{\lambda_0(t)}\sum_k\beta_k z_k(t)} f_{Z_k}(z_k(t))dz_k(t)$$
$$= e^{-\frac{\gamma_{ut}\sigma^2}{\lambda_0(t)P}}\int_0^{A_1} e^{-\frac{\gamma_{ut}}{\lambda_0(t)}\sum_k\beta_k z_k(t)}\frac{2}{\lambda_{h_k}\lambda_{g_k}(t)} \cdot K_0\left(2\sqrt{\frac{z_k(t)}{\lambda_{h_k}\lambda_{g_k}(t)}}\right)dz_k(t)$$
$$= e^{-\frac{\gamma_{ut}\sigma^2}{\lambda_0(t)P}}\prod_{k=1}^{K(t)}\frac{2}{\lambda_{h_k}\lambda_{g_k}(t)}\int_0^{A_1} e^{-\frac{\gamma_{ut}}{\lambda_0(t)}\beta_k z_k(t)} \cdot K_0\left(2\sqrt{\frac{z_k(t)}{\lambda_{h_k}\lambda_{g_k}(t)}}\right)dz_k(t) \tag{20}$$

The integral part of (20) can be solved by Gaussian Chebyshev quadrature (GCQ) [26]. Applying GCQ method, we obtain:

$$I_3 = \frac{\pi\gamma_{Tt}}{M}\left(\sum_{j\neq k}\beta_j|h_j|^2|g_j(t)|^2 + \sigma^2/P\right)e^{-\frac{\gamma_{ut}\sigma^2}{\lambda_0(t)P}}\prod_{k=1}^{K(t)}\frac{1}{\lambda_{h_k}\lambda_{g_k}(t)}\sum_{m=1}^{M}\sqrt{1-\zeta_m^2} \tag{21}$$
$$\cdot\, e^{-\frac{\gamma_{ut}\beta_k(\sum_{j\neq k}\beta_j|h_j|^2|g_j(t)|^2+\sigma^2/P)\gamma_{Tt}(\zeta_m+1)}{2\lambda_0(t)}} \cdot K_0\left(\sqrt{\frac{2\gamma_{Tt}(\sum_{j\neq k}\beta_j|h_j|^2|g_j(t)|^2+\sigma^2/P)(\zeta_m+1)}{\lambda_{h_k}\lambda_{g_k}(t)}}\right)$$

Where, $\zeta_m = \cos\left(\frac{(2m-1)}{2M}\pi\right)$. Therefore $I_2 = I_1 - I_3$ and the outage probability of the selected K tags is given by:

$$P_{out,T_k} = 1 - I_1 + I_3. \tag{22}$$

In the next section, we carry out the performance evaluation through a combination of closed-form mathematical analysis and Monte Carlo simulations to validate the derived expressions.

5. RESULTS AND DISCUSSION

In this section, numerical results are presented to assess the performance of proposed AmBC system and verify the accuracy of our theoretical analysis. The results are compared against theoretical expressions derived in previous sections. Unless stated otherwise, the parameters used in the simulations for generating the plots are as follows: Number of iterations $T = 10^6$, $N = 10, K(t) = 3, R_u = 1, R_T = 0.1$, $\sigma^2 = -90dBm, \alpha = 3, v(t) = 1m/s, \tau = 0.1, \lambda_0(t) = 0.9, \lambda_{h_k} = [0.9, 0.7, 0.6]$, $\lambda_{g_k}(t) = [0.63, 0.45, 0.36]$ and $M = 10$.

Figure 1 compares the performance of static and mobile users under the same tag density and system parameters. The mobile user employs the adaptive selection strategy proposed in section 3, where as the static user relies on a fixed set of tags. The results show that the adaptive mobile user achieves lower outage performance, specially at higher transmit power levels. This is due to the dynamic evaluation of RSS and interference, that allows the mobile user to select stronger and less interfering tags depending on its instantaneous location.

Figure 2 shows the outage probability of the user and three selected tags as a function of the transmit power P, under a fixed reflection coefficient of $\beta_k = 0.3$. The curves for both simulated and analytical results are shown for verification. As transmit power increases, the outage probability of both the user and the tags declines, showing better reliability at higher SNR regimes. There is a close agreement between the analytical and simulation curves, confirming the accuracy of the derived theoretical formulas for the user and tags under moderate interference.

In Figure 3, the impact of the reflection coefficient on outage performance is evaluated. As β increases, the strength of the backscattered signal improves, resulting in enhancing the ability of the user to decode the tags' messages. However, larger values of β also lead to increased interference at the user when decoding the signals. This trade-off is reflected in the figure, where user outage initially is low for lower values of β, but starts rising as β increases. Tags, on the other hand, benefit more consistently from higher reflection coefficient as their RSS becomes more robust against noise and residual interference, and thus their outage drops.

Finally, Figure 4 explores the variation of user outage as a function of the reflection coefficient in both mobile and static environments. The mobile user demonstrates better performance over a wider range of β, showing the benefit of adaptive selection. The mobile user regularly updates its tag selections to stay within the SIC feasibility region, thereby sustaining communication performance even when interference increases.

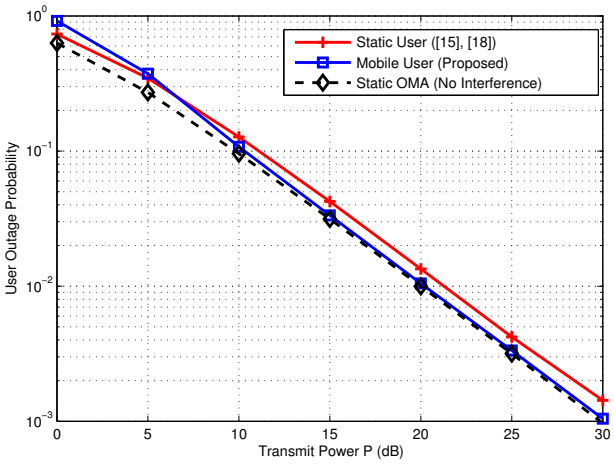

Figure 1. Outage performance of static vs mobile user

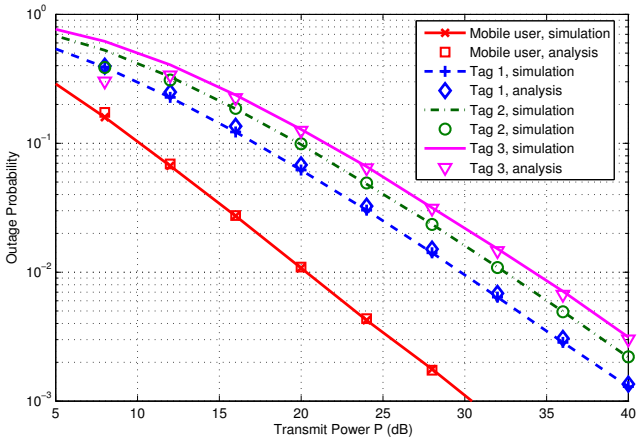

Figure 2. Outage performance versus BS transmit power P for $\beta = 0.3$

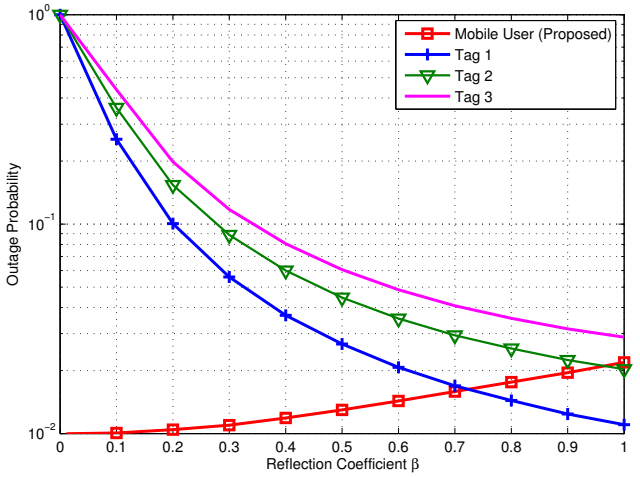

Figure 3. Outage performance versus reflection coefficient β when $p = 20\ dB$

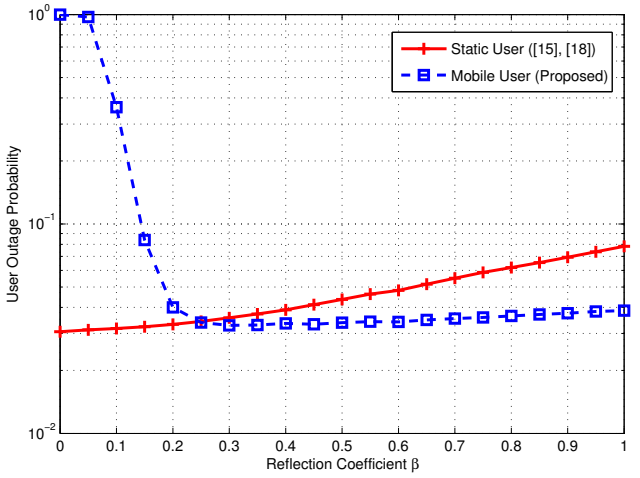

Figure 4. Outage performance of static and mobile users vs reflection coefficient, $P = 15\ dB$

6. CONCLUSION

This paper has presented a detailed analysis and framework for adaptive tag selection in ambient backscatter systems with a mobile user. A SINR aware and interference limited tag selection scheme was proposed to dynamically choose a subset of tags that maximizes reliability while maintaining decodability under SIC constraints. Using analytical outage models, closed-form expressions for user and tags outage probabilities were derived. Simulation results showed that the proposed adaptive strategy outperforms fixed tag selection in terms of outage probability across varying system parameters. This scheme enables the mobile receiver to maintain high decoding reliability even under increased interference confirming its robustness. These findings are particularly relevant for mobile IoT scenarios such as smart transportation, UAV-assisted data collection, and wearable devices. Our work is limited by one mobile user and the absence of experimental results. These limitation is left for future work. As a next step, future work will focus on integrating learning-based adaptive tag selection in rapidly changing environments, experimental prototyping with mobile readers, and extensions to multi-user ambient backscatter systems to further enhance performance in complex mobile IoT scenarios.

FUNDING INFORMATION

Authors state no funding involved for this work.

AUTHOR CONTRIBUTIONS STATEMENT

This journal uses the Contributor Roles Taxonomy (CRediT) to recognize individual author contributions, reduce authorship disputes, and facilitate collaboration.

Name of Author	C	M	So	Va	Fo	I	R	D	O	E	Vi	Su	P	Fu
Mengistu Abera Mulatu	✓	✓	✓	✓	✓	✓	✓	✓	✓	✓				
Thembelihle Dlamini						✓		✓		✓				
Wiseman Nkosingiphile Nyembe						✓		✓		✓				
Zenzo Polite Ncube			✓			✓				✓				
Asrat Mulatu Beyene						✓		✓		✓				

C : **C**onceptualization
M : **M**ethodology
So : **So**ftware
Va : **Va**lidation
Fo : **Fo**rmal Analysis
I : **I**nvestigation
R : **R**esources
D : **D**ata Curation
O : Writing - **O**riginal Draft
E : Writing - Review & **E**diting
Vi : **Vi**sualization
Su : **Su**pervision
P : **P**roject Administration
Fu : **Fu**nding Acquisition

CONFLICT OF INTEREST STATEMENT

The authors declare that they have no conflict of interest.

DATA AVAILABILITY

Data availability is not applicable to this paper as no new data were created or analysed in this study.

REFERENCES

[1] Cisco, "Cisco annual internet report (2018–2023) white paper," *Cisco: San Jose*, vol. 10, no. 1, pp. 1–35, 2020, [Online]. Available: https://www.cisco.com/c/en/us/solutions/collateral/executive-perspectives/annual-internet-report/white-paper-c11-741490.html.

[2] X. Kang, Y. C. Liang, and J. Yang, "Riding on the primary: a new spectrum sharing paradigm for wireless-powered IoT devices," *IEEE Transactions on Wireless Communications*, vol. 17, no. 9, pp. 6335–6347, Sep. 2018, doi: 10.1109/TWC.2018.2859389.

[3] V. Liu, A. Parks, V. Talla, S. Gollakota, D. Wetherall, and J. R. Smith, "Ambient backscatter: wireless communication out of thin air," in *SIGCOMM 2013 - Proceedings of the ACM SIGCOMM 2013 Conference on Applications, Technologies, Architectures, and Protocols for Computer Communication*, Aug. 2013, pp. 39–50, doi: 10.1145/2486001.2486015.

[4] W. Wu, X. Wang, A. Hawbani, L. Yuan, and W. Gong, "A survey on ambient backscatter communications: Principles, systems, applications, and challenges," *Computer Networks*, vol. 216, p. 109235, Oct. 2022, doi: 10.1016/j.comnet.2022.109235.
[5] S. Zargari, A. Hakimi, F. Rezaei, C. Tellambura, and A. Maaref, "Signal detection in ambient backscatter systems: fundamentals, methods, and trends," *IEEE Access*, vol. 11, pp. 140287–140324, 2023, doi: 10.1109/ACCESS.2023.3341416.
[6] J. Qian, F. Gao, G. Wang, S. Jin, and H. Zhu, "Noncoherent detections for ambient backscatter system," *IEEE Transactions on Wireless Communications*, vol. 16, no. 3, pp. 1412–1422, Mar. 2017, doi: 10.1109/TWC.2016.2635654.
[7] W. Chen, H. Ding, S. Wang, D. B. Da Costa, F. Gong, and P. H. J. Nardelli, "Ambient backscatter communications over NOMA downlink channels," *China Communications*, vol. 17, no. 6, pp. 80–100, Jun. 2020, doi: 10.23919/JCC.2020.06.007.
[8] X. Li et al., "Hardware impaired ambient backscatter NOMA systems: reliability and security," *IEEE Transactions on Communications*, vol. 69, no. 4, pp. 2723–2736, Apr. 2021, doi: 10.1109/TCOMM.2021.3050503.
[9] Y. Zhang, Z. Yang, Y. Feng, and S. Yan, "Performance analysis of cooperative relaying systems with power-domain non-orthogonal multiple access," *IEEE Access*, vol. 6, pp. 39839–39848, 2018, doi: 10.1109/ACCESS.2018.2854774.
[10] M. Elsayed, A. Samir, A. A. A. El-Banna, X. Li, and B. M. Elhalawany, "When NOMA multiplexing meets symbiotic ambient backscatter communication: outage analysis," *IEEE Transactions on Vehicular Technology*, vol. 71, no. 1, pp. 1026–1031, Jan. 2022, doi: 10.1109/TVT.2021.3127043.
[11] U. S. Toro, M. Elsayed, B. M. Elhalawany, and K. Wu, "Performance analysis of intelligent reflecting surfaces in ambient backscattering NOMA systems," *IEEE Transactions on Vehicular Technology*, vol. 73, no. 2, pp. 2854–2859, Feb. 2024, doi: 10.1109/TVT.2023.3314394.
[12] R. Zhong, Y. Liu, X. Mu, Y. Chen, and L. Song, "AI empowered RIS-Assisted NOMA networks: deep learning or reinforcement learning?," *IEEE Journal on Selected Areas in Communications*, vol. 40, no. 1, pp. 182–196, Jan. 2022, doi: 10.1109/JSAC.2021.3126068.
[13] V. D. Tuong and S. Cho, "Deep-learning-based resource allocation for 6G NOMA-assisted backscatter communications," *IEEE Internet of Things Journal*, vol. 11, no. 19, pp. 32234–32243, Oct. 2024, doi: 10.1109/JIOT.2024.3424728.
[14] M. Bacha and B. Clerckx, "Backscatter communications for the internet of things: a stochastic geometry approach," *ArXiv*, 2017, [Online]. Available: http://arxiv.org/abs/1711.07277.
[15] Y. Liu, Y. Ye, G. Yan, J. Ma, and Y. Zhao, "Optimal tag selection scheme for a backscatter communication system over the independent but not necessarily identically distributed Rayleigh fading channels," *Electronics Letters*, vol. 57, no. 7, pp. 306–309, Mar. 2021, doi: 10.1049/ell2.12105.
[16] S. Yadav, R. Gour, D. S. Gurjar, and M. Bhatnagar, "Ambient backscatter communications with multi-tag selection: outage performance analysis," *IEEE Communications Letters*, vol. 28, no. 12, pp. 2884–2888, Dec. 2024, doi: 10.1109/LCOMM.2024.3477726.
[17] H. Yang, H. Ding, and M. Elkashlan, "Opportunistic symbiotic backscatter communication systems," *IEEE Communications Letters*, vol. 27, no. 1, pp. 100–104, Jan. 2023, doi: 10.1109/LCOMM.2022.3202362.
[18] Q. Zhang, L. Zhang, Y. C. Liang, and P. Y. Kam, "Backscatter-NOMA: a symbiotic system of cellular and internet-of-things networks," *IEEE Access*, vol. 7, pp. 20000–20013, 2019, doi: 10.1109/ACCESS.2019.2897822.
[19] M. A. Mulatu, T. Dlamini, Z. P. Ncube, and W. Nyembe, "Ambient backscatter communication of passive tags," in *2025 International Conference on Electrical, Computer and Energy Technologies (ICECET)*, 2025, pp. 1–7.
[20] S. Abdallah, M. Saad, and M. Albreem, "Enhanced channel estimation for multi-tag ambient backscatter communication systems," in *2024 7th International Conference on Signal Processing and Information Security, ICSPIS 2024*, Nov. 2024, pp. 1–5, doi: 10.1109/ICSPIS63676.2024.10812591.
[21] S. Ma, G. Wang, R. Fan, and C. Tellambura, "Blind channel estimation for ambient backscatter communication systems," *IEEE Communications Letters*, vol. 22, no. 6, pp. 1296–1299, Jun. 2018, doi: 10.1109/LCOMM.2018.2817555.
[22] F. Baccelli, B. Blaszczyszyn, F. Baccelli, and B. Blaszczyszyn, *Stochastic Geometry and Wireless Networks*, vol. 2. 2009.
[23] M. Haenggi, *Stochastic Geometry for Wireless Networks*, vol. 9781107014. Cambridge University Press, 2012.
[24] D. Li, W. Peng, and F. Hu, "Capacity of backscatter communication systems with tag selection," *IEEE Transactions on Vehicular Technology*, vol. 68, no. 10, pp. 10311–10314, Oct. 2019, doi: 10.1109/TVT.2019.2936648.
[25] I. Gradshteyn and I. Ryzhik, *Table of Integrals, Series, and Products*, 7th ed. London: Academic press, 2007.
[26] F. B. Hildebrand, *Introduction to numerical analysis*. New York, NY,USA, 1987.

BIOGRAPHIES OF AUTHORS

Mengistu Abera Mulatu, member IEEE, received his Ph.D. in Electrical Engineering from the National Taiwan University of Science and Technology, Taipei, Taiwan, in January 2015, M.Sc. degree in Electrical Engineering from Addis Ababa University, Ethiopia, in 2007, and a B.Tech. degree in Electrical Engineering from the Defence University, Ethiopia, in 2002. From December 2002 to July 2008, he worked at the Defence University College, Ethiopian Airlines, and Menschen für Menschen Foundation, Ethiopia. From August 2008 to January 2012, he was a Lecturer at the Institute of Technology, Haramaya University, Ethiopia. He is currently a Senior lecturer in the Department of Electrical and Electronic Engineering at the University of Eswatini. His research interests include cooperative communications, energy harvesting technologies, backscatter communication systems, IoT, 5G/6G, NOMA systems, machine learning and AI-driven wireless systems. He can be contacted at email: mamulatu@uneswa.ac.sz.

Thembelihle Dlamini (Marie Curie Fellow) received his Ph.D. in Information Engineering (Specializing in Information and Communication Technologies (ICT)) from the University of Padova (Italy) in 2020, M.Sc. in Electrical Engineering and Computer Science at National Chiao-Tung University (2014), and a B.Eng degree in Electronic Engineering in 2011. He is currently a Senior lecturer in the Department of Electrical and Electronic Engineering at the University of Eswatini. His research interests include edge computing, machine learning, 5G/6G, and public safety. He can be contacted at email: tldlamini@uneswa.ac.sz.

Wiseman Nkosingiphile Nyembe received his M.Sc. in Electrical Engineering from the University of Cape Town and a B.Eng. degree from University of Eswatini. He is a lecturer in Electrical and Electronic Engineering at the University of Eswatini. His work spans electrical/electronic systems, ICT infrastructure, and programme development, with contributions to curriculum design, accreditation, and national capacity-building initiatives. He is currently pursuing a Ph.D. at the University of Johannesburg, focusing on 6G wireless communications and future connectivity systems. He can be contacted at email: wnyembe@uneswa.ac.sz.

Zenzo Polite Ncube received his Ph.D. in Computer Science in 2012 from the University of South Africa, M.Sc. in Computer Science from NUST, Zimbabwe in 2002, and undergraduate degree in Mathematics and Computer Science from ISP Carlos Manuel De Cespedes in Cuba in 1996 as well as an LLB from the University of South Africa in 2021. He is currently a Senior Lecturer in the Department of Computer Science at the University of Eswatini. He has taught at a number of universities in South Africa including UMP, SPU, NWU and others and his research interests include cyber security and digital forensics, educational technology in higher education, machine learning and AI applications, cellular automata theory, and data science. He can be contacted at email: zenzopn@gmail.com.

Asrat Mulatu Beyene received his M.Sc. from the School of Electrical and Computer Engineering, and his Ph.D. in Wireless Communications Systems of IT Doctoral Program both at Addis Ababa University. Currently, he is working as Associate Professor in the Department of Electrical and Computer Engineering of Addis Ababa Science and Technology University. His research interest spans secure distributed systems and wireless networks, among others. He has secured many international research and national consultancy projects that are impactful and significant. He has published on numerous conference proceedings and journal publications. Besides, he is serving as the President of Internet Society Ethiopian Chapter. He can be contacted at email: asrat.mulatu@aastu.edu.et.